Thallium as a Tracer of Fluid-Rock Interaction in the Shallow Mariana Forearc

Sune G. Nielsen[1*], Frieder Klein[2], Tristan Kading[1], Jerzy Blusztajn[1] and Katie Wickham[3]

[1] – NIRVANA laboratories, Department of Geology and Geophysics, Woods Hole Oceanographic Institution, 02543 Woods Hole, MA, USA

[2] – Department of Marine Chemistry and Geochemistry, Woods Hole Oceanographic Institution, 02543 Woods Hole, MA, USA

[3] – Department of Geology, University of Nevada at Reno, 89557 Reno, NV, USA

Highlights:

- Thallium isotopes record distinct alteration events in the Mariana forearc
- Forearc serpentinization is driven by fluids derived from pelagic sediments
- Diabase underwent rodingitization in the forearc mantle
- Simultaneous serpentinization and rodingitization produces hybrid fluids

Keywords:
Serpentinization, thallium isotopes, Mariana forearc, hydrothermal alteration, rodingitization, subduction

* - corresponding author: snielsen@whoi.edu

Abstract - Fluids driven off the subducting Pacific plate infiltrate the shallow Mariana forearc and lead to extensive serpentinization of mantle peridotite. However, the sources, pathways, and chemical modifications of ascending, slab-derived fluids remain poorly constrained and controversial. In this study, we use thallium (Tl) concentrations and isotopic ratios of serpentinized peridotite and rodingitized diabase from the South Chamorro and Conical Seamounts to discriminate between potential fluid sources with distinct Tl isotope compositions. Serpentinite samples from the Mariana forearc all display ε^{205}Tl > -0.5 (where $\varepsilon^{205}\text{Tl} = 10{,}000 \times ({}^{205}\text{Tl}/{}^{203}\text{Tl}_{\text{sample}} - {}^{205}\text{Tl}/{}^{203}\text{Tl}_{\text{SRM 997}})/({}^{205}\text{Tl}/{}^{203}\text{Tl}_{\text{SRM 997}})$), which is significantly enriched in ^{205}Tl compared to the normal mantle (ε^{205}Tl = -2). Given that high temperature hydrothermal processes do not impart significant Tl isotope fractionation, the isotope compositions of the serpentinites must reflect that of the serpentinizing fluid. Pelagic sediments are the only known slab component that consistently display ε^{205}Tl > -0.5 and, therefore, we interpret the heavy Tl isotope signatures as signifying that the serpentinizing fluids were derived from subducting pelagic sediments. A rodingitized diabase from Conical Seamount was found to have an ε^{205}Tl of 0.8, suggesting that sediment-sourced serpentinization fluids could also affect diabase and other mafic lithologies in the shallow Mariana forearc. Forearc rodingitization of diabase led to a strong depletion in Tl content and a virtually complete loss of K, Na and Rb. The chemical composition of hybrid fluids resulting from serpentinization of harzburgite with concomitant rodingitization of diabase can be highly alkaline, depleted in Si, yet enriched in Ca, Na, K, and Rb, which is consistent with the composition of fluids emanating from mud volcanoes in the Mariana forearc. Our study suggests that fluid-rock interactions between sedimentary, mafic, and ultramafic lithologies are strongly interconnected even in the shallowest parts of subduction zones. We conclude that transfer of fluids and dissolved elements at temperatures and pressures below 400°C and 1GPa, respectively, must be taken into account when elemental budgets and mass transfer between the subducting plate, the forearc, the deep mantle and the ocean are evaluated.

1. Introduction

Oceanic plate subduction releases aqueous fluids into the overriding mantle wedge. Mantle rocks (peridotite, pyroxenite) are unstable in the shallow forearc in the presence of fluids at temperatures lower than ca. 560°C and will undergo hydration and oxidation reactions that are collectively known as serpentinization. Evidence for active serpentinization in the forearc mantle is found at the Mariana forearc, where serpentinite mud, which consists of serpentinite particles suspended in upwelling aqueous fluid, rises along extensional faults and extrudes at the seafloor (Fryer et al., 1985; Mottl et al., 2004). Over time, these mud flows form large serpentinite mud volcanoes that reach diameters and heights of 55 km and 2.5 km, respectively (Fryer, 2012). The extruding mud carries large clasts (up to >1m in diameter (Salisbury et al., 2002)) of partially to completely serpentinized forearc peridotite and a variety of other, less abundant lithologies, including metamorphosed island arc basalt, boninite, mid-ocean ridge basalt, and metamorphic schists (Fryer et al., 2006; Fryer et al., 1999; Johnson and Fryer, 1990; Pabst et al., 2012). Petrologic studies of minerals in metabasites (lawsonite, aragonite, sodic pyroxene and amphibole) suggest that these samples were metamorphosed under blueschist facies conditions at 150-250 °C and 5-6 kbar corresponding to 16-20 km depth and may originate from multiple sources (Maekawa et al., 1993). Since lithologies from the slab-mantle interface (décollement) and slab fluids are otherwise inaccessible by current in situ sampling techniques (drilling), serpentinite mud volcanism provides the best available means to better constrain alteration processes, fluid sources, and pathways within the shallowest portion of the Mariana subduction zone (e.g. Fryer, 2012).

The juxtaposition of subducting altered oceanic crust, sediment, and forearc mantle peridotite creates chemical disequilibria. Fluids driven off the subducting plate can mediate mass transfer through metasomatism along geochemical potential gradients and promote dissolution-precipitation reactions that alter the composition and mechanical properties of rocks. These rocks are either dragged deeper into the subduction zone, where they undergo higher grade metamorphism and possible partial melting, or they are entrained in buoyantly rising serpentinite mud that brings them back towards the surface (Fryer, 2012).

Serpentinization and chemical exchange reactions with mafic and sedimentary lithologies at or near the décollement can alter the composition of the fluids traversing this region. These fluids may then migrate upwards along extensional faults and, ultimately, exit the seafloor into the ocean. Upwelling fluids sampled at the South Chamorro and Conical seamounts have low chlorinities (260-542 mmol/kg) and high alkalitinies (up to 62 mEq/kg, Mottl et al., 2004). Relative to seawater, these fluids are depleted in dissolved Mg, Li, Sr and Ca, but enriched in K, Rb, Cs, and B (Mottl et al., 2004). The high pH (>12) and low concentrations of dissolved silica measured in upwelling fluids (Mottl et al., 2004) are consistent with buffering by serpentine, brucite and diopside during serpentinization at temperatures lower than 300°C (Klein et al., 2013). However, the upwelling fluid's enrichment in alkali metals relative to seawater cannot be explained by serpentinization of alkali-poor mantle peridotite alone, which indicates that additional processes affected these fluids before they were expelled at the seafloor. The lower chlorinity of the emitted fluids has been attributed to dehydration reactions within the subducting plate, as opposed to compaction of sediments, which is thought to produce fluids with chlorinities similar to that of seawater (Mottl et al., 2004). However, the source of the fluid responsible for forearc serpentinization remains controversial. For example, chlorine isotopes of serpentinite muds and clasts from Conical, South Chamorro and Torishima seamounts suggest that dehydration of subducted oceanic serpentinite is one potential fluid source (Barnes et al., 2008). Conversely, evidence from O and H isotopes in serpentine samples was inferred to suggest that seawater and altered oceanic crust are likely fluid sources (Sakai et al., 1990). In contrast to both prior hypotheses, it was argued that subducted sediments are the fluid source for serpentinization of the forearc mantle (Alt and Shanks, 2006), which was based primarily on O and H isotopes in serpentinites from South Chamorro and Conical seamounts. The main difficulty in these previous studies was that 1) the temperature of fluid release imparts a strong influence on its O and H isotopic characteristic, 2) the isotopic endmembers for the different fluid sources may overlap and 3) a significant spread in the serpentinite isotopic data made it difficult to pinpoint the exact fluid source.

The thallium (Tl) isotopic composition of the Earth's mantle and unaltered oceanic basement is homogenous (ε^{205}Tl = -2) and differs significantly from that of isotopically heavier pelagic sediments

(ε^{205}Tl = 0 to 5, n = 5) and isotopically lighter low-temperature altered oceanic crust (ε^{205}Tl = -15 to -2, n = 30) (Fig. 1). In addition, the concentration of Tl found in sediments and low-temperature (low-T) altered oceanic crust is up to four orders of magnitude higher than that found in the mantle and unaltered oceanic crust (Coggon et al., 2014; Heinrichs et al., 1980; Nielsen et al., 2006c; Nielsen et al., 2014; Rehkämper et al., 2004; Teagle et al., 1996). Thus, if serpentinizing fluids are derived from either pelagic sediments or low-T altered oceanic crust, then Tl isotopes should be ideally suited to distinguish fluids derived from devolatilization of either source during subduction. Here we use Tl concentrations and isotope ratios of samples recovered during ODP Legs 125 and 195 from the Conical and South Chamorro seamounts as a tracer of fluid sources and metasomatic mass transfer in the shallow Mariana forearc.

2. Thallium isotopic background

Thallium is a trace metal that displays both lithophile and chalcophile behavior. In geochemistry, it is often grouped with the alkali elements K, Rb, and Cs due to their similar ionic radii and charge (Heinrichs et al., 1980; Shannon, 1976; Shaw, 1952). Thallium is incompatible during mantle melting and is enriched in the continental crust (~300-500 ng/g) relative to the mantle (~0.5-2 ng/g) (Heinrichs et al., 1980; Nielsen et al., 2005; Nielsen et al., 2014; Wedepohl, 1995). Adsorption leads to Tl enrichment in pelagic metalliferous sediments (~750-3500 ng/g) and deposition of alteration minerals from mobile fluid phases increases Tl concentrations in low temperature hydrothermally altered seafloor basalts (~30-1000 ng/g) (Coggon et al., 2014; Nielsen et al., 2006c; Prytulak et al., 2013; Rehkämper et al., 2004).

Thallium has two stable isotopes with masses 203 and 205. Thallium isotope compositions are reported relative to the NIST SRM 997 Tl standard in parts per 10,000 such that

$$\varepsilon^{205}\text{Tl} = 10{,}000 \text{ x } ({}^{205}\text{Tl}/{}^{203}\text{Tl}_{\text{sample}} - {}^{205}\text{Tl}/{}^{203}\text{Tl}_{\text{SRM 997}})/({}^{205}\text{Tl}/{}^{203}\text{Tl}_{\text{SRM 997}}) \quad (1)$$

The small relative mass difference between the two isotopes prevents extensive isotopic fractionation except in select environments where nuclear volume isotope fractionation occurs during chemical reactions primarily involving both oxidation states of Tl, +1 and +3 (Nielsen and Rehkämper, 2011; Schauble, 2007). However, trivalent Tl is not thermodynamically stable in igneous environments, and Tl dissolved in seawater is almost exclusively univalent (Byrne, 2002; Nielsen et al., 2009a). The uniform Tl redox state of the mantle renders the average upper mantle homogenous with respect to Tl isotopes (ε^{205}Tl = -2 ± 0.5) with no significant isotope fractionation expected during melting or fractional crystallization (Schauble, 2007). In contrast, hydrothermally altered oceanic crust and metalliferous marine sediments are highly variable with respect to Tl isotope ratios and concentrations.

Enrichment of Tl in marine sediments is primarily due to adsorption onto authigenic manganese (Mn) oxides (Hein et al., 2000; Nielsen et al., 2013; Rehkämper et al., 2004; Rehkämper et al., 2002) that precipitate ubiquitously from oxic seawater onto sedimentary particles. Mn oxides preferentially take up ^{205}Tl with a fractionation factor of up to $\alpha = 1.002$ (Nielsen et al., 2013; Rehkämper et al., 2004; Rehkämper et al., 2002), although such high fractionation factors are only observed for pure hydrogenetic ferro-manganese crusts that can have isotope compositions as high as ε^{205}Tl ~ +15 (Rehkämper et al., 2004). This adsorption process is responsible for heavy Tl isotope compositions detected in pelagic clays (Rehkämper et al., 2004).

In the basaltic oceanic crust, Tl enrichment occurs during the circulation of seawater at low temperatures (<100°C). The thallium enrichment may be related to biologically mediated pyrite precipitation (Coggon et al., 2014) or alternatively Tl partitions from circulating seawater into alkali-rich clay minerals that also form during low-T alteration (Nielsen et al., 2006c). Analysis of Tl concentrations and isotopes in low-T altered crust from IODP Hole U1301B, Deep Sea Drilling Project (DSDP) Hole 417D and DSDP/Ocean Drilling Program (ODP) Hole 504B showed high Tl concentrations (30-1000 ng/g) and light Tl isotope ratios (down to ε^{205}Tl ~ -15; (Coggon et al., 2014; Nielsen et al., 2006c)).

In high-temperature hydrothermal systems, Tl preferentially partitions into the fluid phase over the rock during reaction. Typical MORB has a Tl abundance of about 10 ng/g (Nielsen et al., 2014), while seawater concentrations are ~10-15 pg/g Tl (Flegal and Patterson, 1985; Nielsen et al., 2006c), and black smoker type hydrothermal vent fluids contain around 5 ng/g (Metz and Trefry, 2000; Nielsen et al., 2006c). The ~500-fold disparity in Tl concentration between seawater entering the hydrothermal system and the hydrothermal vent fluid discharged into the ocean requires that virtually all of the aqueous Tl present was derived from water-rock interaction.

The sheeted dike portion of the oceanic crust has low Tl concentrations (<1 ng/g; (Nielsen et al., 2006c)) that reflects the leaching by high temperature hydrothermal fluids (200-400°C) near the ridge axis. This removal of Tl does not result in isotope fractionation and the sheeted dikes have a ε^{205}Tl similar to MORB glass (ε^{205}Tl ~ -2 ± 0.5; (Nielsen et al., 2006b; Nielsen et al., 2006c)). Black smoker fluids also display Tl isotope compositions that are identical to MORB and the upper mantle, which shows that there is no detectable isotope fractionation between high-T fluids and the altered basalts that reacted with these fluids (Nielsen et al., 2006c). This relationship is consistent with theoretical calculations of Tl isotope fractionation, which predict negligible effects at T>200°C, especially at reducing conditions typical for high temperature hydrothermal alteration and serpentinization processes where dissolved trivalent Tl is not stable (Nielsen et al., 2009a; Schauble, 2007). Serpentinization in the forearc occurs at temperatures comparable to those found in recharge zones and cooler parts of reaction zones of high-temperature black smoker type hydrothermal systems (200-400°C), which may suggest that Tl will partition between fluid and rock similarly in both settings. This inference is corroborated by analyses of serpentinites from both forearc and mid-ocean ridge settings where Tl concentrations are similar to the sheeted dike complex (Kodolanyi et al., 2012), which shows that Tl partitions similarly between rock and fluid in both types of high-temperature hydrothermal systems. Compared to basalt alteration at mid-ocean ridges, however, forearc serpentinization is characterized by some important differences. First, unaltered mantle rocks contain more than an order of magnitude less Tl than MORB because Tl is strongly incompatible during mantle melting (Nielsen et al., 2014). Moreover, the composition of the original serpentinizing fluid before interaction with mantle rocks is very different from seawater because it is likely derived from subducting sediments and/or altered oceanic basement (Alt and Shanks, 2006; Mottl et al., 2004; Sakai et al., 1990).

Although the exact concentration of Tl in the serpentinizing fluid is unknown, it is almost certainly higher than seawater because it interacted with either basalt or sediment, which contain at least 1000 times more Tl than seawater per unit volume, at temperatures above 150°C (Alt and Shanks, 2006; Mottl et al., 2004). Considering these differences, it appears likely that the slab-derived fluid dominates the total Tl budget of forearc serpentinization. This means that we would expect serpentinites to exhibit the Tl isotope composition of the fluids derived from the slab component that caused the serpentinization.

3. Samples and methods

3.1. Samples

We investigated Tl isotopes and concentrations in nine partially to completely serpentinized peridotites and one rodingite from the ODP Holes 779A and 1200A. Thin section petrography revealed that all protoliths can be classified as harzburgite except the rodingite, which was likely diabase (Johnson, 1992).

In the serpentinites, all primary silicates are fractured with sub-grainsizes ranging between <50µm and several hundred µm. Olivine is partly to completely altered to serpentine (lizardite and minor chrysotile) > brucite > Ni-Fe sulfides / alloy > magnetite in mesh, hourglass and ribbon textures. All examined rocks are generally magnetite-poor. Only a few transgranular veins in samples 1200A-3R-1W, 3-7cm, 1200A 11R-1W, 47-49cm, and 779A-35R-1W, 22-24cm contain minor (maximum a few percent) amounts of magnetite (Fig. 2). Orthopyroxene is partly to completely altered to lizardite and minor chlorite in bastite texture. Bastite contains neither talc nor magnetite. One sample from Conical seamount (779A-35R-1W, 22-24cm) contains antigorite-brucite assemblages interpreted to have formed at the expense of lizardite during prograde metamorphism. In contrast to the brown, Fe-bearing brucite in mesh texture, the brucite associated with antigorite in interpenetrating texture is colorless and Fe-poor (Murata et al., 2009). All of the samples examined in this study show several vein generations, with earlier veins consisting chiefly of lizardite and late veins consisting of chrysotile (Kahl et al., 2015). Chrysotile veins cross-cut antigorite blades in sample 779A-35R-1W, 22-24cm, suggesting these veins postdate prograde metamorphism. Iron-rich brucite and iowaite precipitated late in veins and mesh texture (Fig. 2), which led to a brownish overprint in several clasts (Kahl et al., 2015). Clinopyroxene (diopside) is the least abundant primary silicate in all serpentinite samples examined in this study. Where present, it occurs as subhedral crystals, as symplectite intergrown with Cr-spinel or as exsolution lamellae in orthopyroxene. In most instances, clinopyroxene has remained largely unaltered. In some completely altered orthopyroxene grains, the clinopyroxene exsolution lamellae appear to have been altered to chlorite. Chromium spinel is fractured and, in many instances, shows thin alteration rims consisting of ferri-chromite.

One rodingite recovered from Conical seamount was analyzed in this study. Johnson (1992) performed major and trace element analyses of 6 subsamples from the same interval and found it to be homogenous. Consistent with previous findings (Johnson, 1992), the sample analyzed here consists of primary and secondary clinopyroxene and andradite-rich hydro-garnet, minor chlorite, pumpellyite, and traces of relict sphene (Fig. 2). We also analyzed one completely serpentinized peridotite from the Mid-Atlantic Ridge Kane (MARK) Fracture Zone area, which was recovered during ODP Leg 153 (920B-12R-2W, 140-143 cm). This particular sample consists chiefly of Fe-bearing serpentine ($X_{Mg} \approx 0.95$) and brucite ($X_{Mg} \approx 0.90$); It is rich in magnetite (6.15 wt%) and likely formed at temperatures ≥250°C (Klein et al., 2014). In addition, we analyzed one unaltered harzburgite xenolith from the Meerfelder Maar (Eifel Volcanic Field, Germany, see Klein et al., (2015) for detailed petrographic description and chemical analyses) in order to compare unaltered mantle peridotite and abyssal serpentinite with those from the Mariana forearc.

3.2. Sample preparation

All samples were cut into cm-sized pieces using a diamond saw blade and ca. 5-10g were powdered with a disc grinder in a tungsten carbide (WC) barrel. The WC barrel was cleaned with high purity quartz before and after each run, triple rinsed with deionized water and air dried to avoid cross-contamination. Contamination of Tl from the WC barrel is highly unlikely given that different samples (e.g. 920B-12R-

2W, 140-143 cm and 10R-2W, 51-53cm) with very low Tl concentrations display Tl isotope compositions that are very different. Thus, any Tl contamination from the WC barrel must be significantly smaller than the 0.14 ng/g observed in 10R-2W, 51-53cm. Powdered samples (1 - 5 g) were dissolved in ~5ml/g of a 1:1 mixture of concentrated HF and HNO_3 on a hotplate overnight. Following this, they were dried and fluxed several times with concentrated nitric acid and hydrochloric acid until the fluorides that formed during the first step could no longer be seen. After these steps, some samples still contained a minor amount of undissolved spinel. However, spinel does not contain detectable amounts of Tl (Nielsen et al., 2014) so these residues had no effect on our Tl isotope and concentration analyses. Following complete dissolution of fluorides, the samples were dissolved in ~1 M HCl and MQ water saturated in bromine was added to oxidize Tl to the trivalent oxidation state (Nielsen et al., 2004; Rehkämper and Halliday, 1999). A two-stage column chromatographic technique with anion-exchange resin was used to isolate Tl from rock samples (Nielsen et al., 2004; Nielsen et al., 2005). This procedure has been shown to produce quantitative yields for Tl (Nielsen et al., 2004; Nielsen et al., 2006a; Rehkämper et al., 2004). Total procedural Tl blanks during this study were <3pg, which is insignificant compared to the indigenous Tl processed for the samples. We processed >250pg Tl for all samples, with the majority containing >1ng.

3.3. Determination of Tl isotope compositions and concentrations

The Tl isotope compositions were determined at the WHOI Plasma Mass Spectrometry Facility using a Thermo Neptune multiple collector inductively coupled plasma-mass spectrometer (MC-ICPMS). Previously described techniques that utilize both external normalization to NIST SRM 981 Pb and standard-sample bracketing were applied for mass bias correction (Nielsen et al., 2004; Rehkämper and Halliday, 1999). Due to the quantitative yields of Tl from the column chemistry procedure, Tl concentrations could be determined by monitoring the ^{205}Tl signal intensities of the samples during the isotopic measurements. A known quantity of NIST SRM 981 Pb was added to the sample Tl and the measured ^{205}Tl/^{208}Pb ratios were then converted directly into Tl abundances. Previous studies that utilized the Nu Plasma MC-ICPMS applied a 5% correction that assumed Tl ionizes 5% more efficiently than Pb. However, we have not been able to verify this behavior for the Neptune and thus do not apply this correction here. The uncertainty on the Tl concentration measurements is likely on the order of ±10% (2sd) (Prytulak et al., 2013). Our new data for 10 separate digestions of the USGS reference basalt BHVO-1 (Table 1) exhibited [Tl] = 37 ± 4 ng/g (2sd), which is in good agreement with several previous studies that found values of 38 ± 4 ng/g (Prytulak et al., 2013) and 40 ± 5 ng/g (Makishima and Nakamura, 2006).

The precision and accuracy of the Tl isotope measurements has been investigated in previous studies (Nielsen et al., 2004; Rehkämper and Halliday, 1999), even for samples with low abundances of Tl (Nielsen et al., 2006a). During the course of this study, we used the long-term reproducibility of BHVO-1 (Table 1) to assess our external error on unknown samples and found ε^{205}Tl = -3.5 ± 0.5 (2sd). We apply this uncertainty to all measurements that were conducted using total Tl ion beams in excess of 1.5×10^{-11} A, whereas samples with total Tl ion beams $<0.7 \times 10^{-11}$ A and between 0.7 and 1.5×10^{-11} A were assigned errors of ±1 and ±0.8 ε^{205}Tl-units, respectively, in accordance with previous studies (Nielsen et al., 2007; Nielsen et al., 2009b).

3.4. Other analytical work

The major and trace element contents of whole rock samples (Table 2) were analyzed by XRF in the Peter Hooper GeoAnalytical Laboratory at Washington State University (Pullman, WA) using previously described methods (Johnson et al., 1997). Thin sections were examined using a petrographic microscope in transmitted and reflected light. Where minerals could not be unequivocally identified, thin sections were analyzed with a Horiba Labram HR confocal Raman spectrometer equipped with a 17 mW 633 nm HeNe laser, a 25mW 473 nm diode-pumped solid state laser, an astigmatic flat field spectrograph with a focal length of 800 mm, and a multichannel air-cooled (-70 °C) CCD detector. Individual spectra were recorded using a 100x objective with a numerical aperture of 0.9. A grating with 600 grooves / mm and a confocal hole diameter of 100 to 200 µm was chosen for most analyses. Spectra were collected for 5 seconds with 3-5 accumulations between 100 cm^{-1} and 1300 cm^{-1} and for 20 seconds between 3500 cm^{-1} and 3800 cm^{-1}. Confocal Raman maps were collected with the 473 nm laser between 180 and 2200 cm-1 with a 50x objective and a step size of 2µm. The Horiba SWIFT™ fast mapping option was employed and individual spectra were recorded for 0.8 seconds.

4. Results

Serpentinite samples from the Mariana forearc display a range of isotope compositions from ε^{205}Tl = -0.5 to +1.8 (Table 3). Statistically, the samples can be divided into two groups (Student's T-test yields a probability of <0.02% that the two sample populations are from the same group): One that is isotopically heavier with ε^{205}Tl = 1.3 ± 0.7 (2sd), and another isotopically lighter with ε^{205}Tl = -0.3 ± 0.7 (2sd). The rodingite sample from ODP Hole 779A, mainly composed of secondary diopside and hydro-andradite, exhibits value most similar to the heavier serpentinites of ε^{205}Tl = +0.8 ± 0.5. In contrast, one serpentinite sample from the Mid-Atlantic Ridge and an unaltered harzburgite from the Meerfelder Maar, Eifel Volcanic Field (Germany) have values within error of ε^{205}Tl = -2.0 ± 0.5, which is the generally accepted value for the upper mantle (Nielsen and Rehkämper, 2011; Nielsen et al., 2007; Nielsen et al., 2006b). Among all of the samples analyzed, the Tl concentrations fall within 0.14 to 1.25 ng/g, which is consistent with the most recent estimate of Tl concentration in the upper mantle of 0.5±0.1 ng/g (Nielsen et al., 2014). There is no noticeable difference in concentration between unaltered harzburgite, rodingite and serpentinized harzburgite from either tectonic setting. The Tl concentrations measured here for serpentinites are similar to those found by Kodolanyi et al. (2012) in serpentinite clasts from various tectonic settings.

Two of the serpentinite samples were run in duplicate through the entire procedure of sample dissolution, Tl separation and mass spectrometry (Table 3). Although the isotopic compositions measured for these duplicates are within analytical error, the concentrations registered for one of the samples are outside of the ±10% uncertainty quoted for our concentration measurements. This discrepancy could have been caused by a small amount of residual fluoride not coming completely into solution due to the relatively large quantity of sample (>1g) required to obtain sufficient Tl for isotopic analysis. Alternatively, it is possible that Tl is heterogeneously distributed in the samples. However, since we do not know the exact mineralogical partitioning of Tl in the serpentinite samples, it is difficult to further assess this hypothesis. In any case, the duplicates confirm that our data are precise and accurate to the quoted long-term reproducibility.

5. Discussion

5.1. Origin of heavy thallium isotopic composition of forearc serpentinites

All serpentinites analyzed from the Mariana forearc display Tl isotopic compositions of ε^{205}Tl > -0.5, which is significantly heavier than normal mantle. This difference indicates that Tl isotope ratios in the harzburgite protolith were altered during serpentinization. The likely high Tl concentrations in the serpentinizing fluids and low Tl concentrations in harzburgites imply that the total Tl budget of the serpentinization system is skewed heavily towards the fluid. In addition, the lack of Tl isotope fractionation between hydrothermal fluid (T ~ 200-400°C) and hydrothermally altered rock (Nielsen et al., 2006c) suggests that the Tl isotope compositions of the serpentinites reflect that of the serpentinizing fluids, and not an isotope fractionation process taking place during serpentinization. On the basis of high B and Li concentrations and unradiogenic Sr isotope compositions of Mariana forearc serpentinites, it was argued that seawater on its own could not represent a major source of serpentinization fluids (Savov et al., 2007). This conclusion is confirmed by our isotopically heavy Tl isotope serpentinite data because open ocean seawater is characterized by ε^{205}Tl = -6 ± 0.5 (Nielsen et al., 2006c; Rehkämper et al., 2002), which is far from all the measured ε^{205}Tl of forearc serpentinite (Table 3). The question then arises as to what the origin of heavy Tl isotope compositions in the serpentinizing fluid is? Thallium isotope fractionation between source rock and serpentinizing fluid is also unlikely given that the extraction of the serpentinizing fluid from the subducting slab likely took place at temperatures similar to that of the serpentinization itself i.e. ~175-240°C (Kahl et al., 2015). Hence, the serpentinizing fluid characterized by ε^{205}Tl > -0.5 must have been derived from a source with similar Tl isotopic composition.

There are multiple possible fluid sources within the subducting slab: previously serpentinized oceanic mantle (Barnes et al., 2008), hydrothermally altered oceanic crust (Sakai et al., 1990), and subducted sediments (Alt and Shanks, 2006). Of these three slab components, only pelagic sediments have been observed to systematically exhibit ε^{205}Tl > -2 (Coggon et al., 2014; Nielsen et al., 2006c; Rehkämper et al., 2004), Table 3), which implies that fluids released from sediments are the most likely source of heavy Tl isotopes measured for Mariana forearc serpentinites.

The oceanic crust and sediments that are being subducted at the Mariana arc (ODP Hole 801C) were previously investigated for Tl isotopes. Analyses of two discrete pelagic clays were rich in Tl (~3000 ng/g) with isotope compositions of ε^{205}Tl = -0.3 and 0.4 (Prytulak et al., 2013). Altered oceanic crust from ODP Hole 801C, on the other hand, was not significantly enriched in Tl compared with fresh basaltic melts and was found to vary from ε^{205}Tl = -4 to 0 (Prytulak et al., 2013). Five serpentinites investigated here are isotopically heavier (ε^{205}Tl > +1) than both sediments and altered oceanic crust from ODP Hole 801C, which makes it unlikely for these bulk components to be the primary source of Tl in the serpentinizing fluid. It should be noted that, as opposed to the nine composite altered oceanic crust samples from ODP Hole 801C that sample averages of the main units in the upper ~400m of low-T altered oceanic crust, only two discrete samples of pelagic sediment from ODP Hole 801C were reported (Prytulak et al., 2013) and it is possible that other pelagic sediment samples from ODP Hole 801C might contain slightly heavier Tl isotope compositions as has been observed for modern pelagic sediments (Rehkämper et al., 2004). The heavy Tl isotope compositions of pelagic sediments reflect the presence of Mn oxides that form as coatings on sediment particles. Sedimentary particles themselves can contain Tl concentrations similar to or higher than continental crust ([Tl] ~ 300-500 ng/g, (Nielsen et al., 2005; Wedepohl, 1995)) and are also characterized by Tl isotope compositions akin to that of the continental crust; ε^{205}Tl ~ -2 (Nielsen et al., 2005). Thus, Mn oxide coatings on pelagic sediment particles are likely isotopically heavier than the bulk sediment. Given that the serpentinizing fluids can be highly reducing (Klein et al., 2013) and that Mn oxides (MnO_2) are readily soluble under reducing conditions because Mn(IV) is reduced to highly soluble Mn(II), it follows that the Mn oxide component of pelagic clays would be preferentially mobilized into the fluid. This process would cause the Tl isotope composition of the fluid to be heavier than the bulk sediment, which may explain why the serpentinizing fluids, as recorded by the serpentinites, appear to have had somewhat heavier Tl isotope compositions than the bulk sediment source.

It should be noted that Cl isotope evidence appear to implicate fluids released from previously serpentinized oceanic peridotites as the source of Cl in forearc serpentinization reactions (Barnes et al., 2008). The Tl isotope evidence presented here, however, does not exclude this possibility because the Tl content of oceanic serpentinites are so low that fluids released from such a rock would likely contain vanishingly small amounts of Tl and therefore not contribute to the Tl budget of these fluids. Serpentinization is associated with chlorine isotope fractionation of ~0.4 permil (Barnes et al., 2008), which would yield $\delta^{37}Cl \sim -0.4$ to 0 for the serpentinizing fluids in equilibrium with the Mariana forearc serpentinites (Barnes et al., 2008). It is particularly noteworthy that pelagic sediments from ODP Holes 800A, 801A and 1149A have some of the highest Cl concentrations (>1%) coupled with the heaviest sediment Cl isotope compositions of $\delta^{37}Cl \sim -0.3$ to -0.7, which is within the expected range for the Cl isotope composition of the serpentinizing fluid. Chlorine isotopic data are therefore equally compatible with pelagic sediments contributing to the serpentinization fluids.

5.2. Light Tl isotopes in brucite/iowaite-bearing serpentinite

Even though the samples analyzed in this study fall into two statistically different groups, it is likely that the relatively dynamic fluid environment of the Mariana forearc will produce a continuum of compositions between the light and the heavy isotope compositions observed. As such, the division of our samples into two groups may be an artifact of the small number samples analyzed. However, it is interesting that the isotopically lighter samples also display the lowest SiO_2 contents (<35%), highest Tl and Zn (not shown) concentrations, and the highest loss on ignition (LOI) >16% (Fig. 3). These relationships suggest that the observed Tl isotopic differences between the two groups were generated by systematic differences in either hydrothermal conditions, like temperature, or fluid compositions.

Serpentine, which is the dominant alteration phase during initial serpentinization near the décollement, can form at relatively high silica activities (Klein et al., 2009). Serpentine contains ~ 42 wt.% SiO_2 and ~14 wt.% H_2O and thus accounts for the majority of water and SiO_2 in most of the serpentinites. Iron-bearing brucite and iowaite, which overprinted the initial serpentinization mineralogy (Fig. 2), contain about 25 to 32 wt.% water, respectively, but no Si. Samples exhibiting $\varepsilon^{205}Tl < +1$ generally contain higher abundances of Fe-bearing brucite and iowaite, which accounts for the higher observed LOI and lower SiO_2 concentrations. However, modal abundances of serpentine, brucite and iowaite vary widely on a thin section scale, making it difficult to directly relate in situ thin section analysis with Tl isotope analysis of bulk samples. Nevertheless, it appears that the decrease in $\varepsilon^{205}Tl$ is related to the event(s) that caused the precipitation of Fe-bearing brucite and/or iowaite. Although Fe-bearing brucite can form at various stages during serpentinization (Beard et al., 2009; Kahl et al., 2015; Klein et al., 2009), its formation generally is indicative of relatively low silica activities (Klein et al., 2009). Because the devolatilization of subducting pelagic clays and altered oceanic crust produces Si-rich fluids, Fe-bearing brucite formation near the décollement is unlikely to occur (cf. Kahl et al., 2015). However, the exact origin of the lighter Tl isotope composition measured for the Si-poor serpentinites is difficult to determine and may be explained by effects from temperature or changing fluid composition.

The maximum temperature of the décollement at 25-30 km depth beneath the South Chamorro and Conical Seamounts is estimated to be 300°C based on thermal models for subduction of old oceanic crust, which is consistent with temperature estimates from petrological phase relations (Fryer et al., 2006; Hyndman and Peacock, 2003). Prograde metamorphism of some but not all serpentinites from Conical Seamount produced antigorite-brucite assemblages, which may reflect somewhat higher temperatures (Evans, 2004). However, the Fe-rich nature of brucite and lack of magnetite in several serpentinites suggest alteration temperatures of less than ca. 200°C (Klein et al., 2014; Klein et al., 2013). Such low temperatures are corroborated by estimates of Kahl et al. (2015), who calculate temperatures of 175 to

240°C on the basis of oxygen-isotope thermometry (assuming the $\delta^{18}O$ of the serpentinization fluid was +2.5‰, (Fryer et al., 2006)). On the other hand, serpentinization fluids emanating from South Chamorro are cool (~2°C) (Fryer et al., 1990; Mottl et al., 2004) implying that hydrothermal alteration reactions in the forearc may span the full temperature range of about 300°C. This inference is supported by the presence of iowaite, which is believed to form at low temperatures (<60°C, (Frost and Erickson, 2004)) and its formation requires the addition of Cl and fairly oxidizing conditions that are not encountered during serpentinization. Heling and Schwarz (1992) analyzed iowaite in serpentinite mud from Conical Seamount and suggest that it forms in seafloor environments where Fe-bearing brucite is exposed to seawater.

Although equilibrium Tl isotope fractionation is predicted to be very small in systems that, like serpentinization, dominantly contain only species of the univalent Tl ion (Table 4 in Schauble, 2007), hydrothermal temperature differences of more than 200°C could result in isotope fractionation factors that differ by more than 1 ε^{205}Tl-unit (Schauble, 2007). Thus, if we assume no change in the Tl isotope composition of the serpentinizing fluid, then a fluid temperature change from 300°C to 50°C could produce rocks that were ~1 ε^{205}Tl-unit lighter, which is consistent with the observed lighter values for samples that contain Fe-rich brucite and iowaite.

Alternatively, if there is little to no Tl isotope fractionation occurring during any of the hydrothermal alteration reactions, then the Tl isotope composition of the serpentinites could reflect different fluid compositions, potentially extracted from separate sources. Large portions of the subducting slab, including detrital/clastic sediments and altered oceanic crust at ODP Hole 801C display $\varepsilon^{205}Tl = -1 \pm 0.5$ (Nielsen et al., 2005; Prytulak et al., 2013), which is similar to the lightest Tl isotope compositions observed for the forearc serpentinites. This value is still outside the composition of serpentinized oceanic mantle, which rules out this component as a significant source of Tl to the serpentinizing fluids.

5.3 Rodingitization in the forearc mantle

Rodingites are Ca-rich, Si- and alkali-poor metasomatic rocks (protoliths can range from mafic to granitic and sedimentary lithologies) that are exclusively associated with serpentinites (Bach et al., 2013; Coleman, 1963, 1977; Frost and Beard, 2007). Consequently, rodingitization is commonly conceptualized as Ca-metasomatism due to the breakdown of clinopyroxene during serpentinization (Coleman, 1963). However, several recent studies have highlighted the important role low silica activities imposed by serpentine-brucite-diopside phase equilibria at T < 330 °C play during rodingitization (Bach et al., 2013; Bach and Klein, 2009; Frost and Beard, 2007; Frost et al., 2008). The low silica activities imposed by serpentinization lead to the removal of Si from the mafic or sedimentary protolith, thereby stabilizing Si-poor Ca-Al silicates, including zoisite, prehnite, (hydro-)grossular/andradite, vesuviante, diopside and chlorite. At higher temperatures (~400°C), serpentinization fluids are buffered by serpentine-talc-tremolite equilibria to significantly higher silica activities. Such fluids cannot form rodingite. Instead, monomineralic chlorite blackwalls form at the expense of mafic lithologies (Bach and Klein, 2009). Thus, rodingite can form wherever mafic lithologies are exposed to Si-poor serpentinization fluids such as along slow- and ultraslow spreading mid-ocean ridges, at continental margins, and in subduction zones. This raises the question as to where the rodingite drilled at Conical seamount originated? It seems unlikely that the rodingite formed in a mid-ocean ridge setting, since the oceanic crust presently subducted beneath the Mariana arc originated from a fast spreading ridge with a full spreading rate 160 mm/a. However, rodingitization at fast spreading ridges may still occur in tectonic windows such as Hess Deep, Equatorial Pacific (Mével and Stadoumi, 1996), where mantle peridotite and mafic lithologies are exposed to seawater. Thus, we cannot rule out that the diabase was originally rodingitized in the Eastern Pacific and then overprinted by sediment derived slab fluids in the Mariana forearc before it emerged at Conical seamount. However, several lines of evidence support the idea that rodingitization took place in situ within the shallow forearc mantle. First, serpentinization is known to take place in the Mariana forearc beneath the Conical and South Chamorro seamounts (Fryer, 2012) at temperatures susceptible to rodingitization (Bach and Klein, 2009). Second, the mafic lithologies of the subducting Pacific plate are in close proximity to the overriding forearc mantle, making interaction between the two possible. Third, rodingitization involves a virtually complete loss of alkalis from the mafic precursor lithologies. Indeed, pore fluids sampled at Mariana forearc mud volcanoes are enriched in alkalis despite being primarily influenced by serpentinization reactions (Hulme et al., 2010; Mottl et al., 2004). Lastly, given that rodingitization is invariably linked to the serpentinization process, the heavy Tl isotope composition of the rodingite implicates a pelagic sediment source for the rodingitization fluid, which cannot have occurred in a mid ocean ridge setting. We, therefore, suggest that rodingitization took place during serpentinization in the forearc mantle. Although it remains unclear where exactly rodingitization took place, it seems likely that it was in a regime where Si activities were relatively low (Bach and Klein, 2009), i.e. not in direct contact with Si-rich pelagic clays that would produce quartz-saturated fluids.

6. Conclusions

Previous studies have highlighted that fluids derived from the subducting Pacific plate are responsible for serpentinization of the forearc mantle, but the fluid sources driving this process, i.e. altered oceanic basement, subducted sediment, or a combination thereof remains controversial (Alt and Shanks, 2006; Barnes et al., 2008; Kahl et al., 2015; Sakai et al., 1990). This study used Tl isotope systematics in serpentinized peridotite from the South Chamorro and Conical seamount to trace fluid-rock reactions in the shallow Mariana forearc. The Tl isotope ratios measured in serpentinite clasts from the South Chamorro and Conical Seamounts were all heavier than the harzburgite protolith, which strongly implicates serpentinization by a fluid extracted from pelagic sediments. A subset of the analyzed serpentinites was characterized by lower SiO_2 concentrations, higher Tl and Zn concentrations, higher LOI, and the lightest Tl isotope compositions (Fig. 3). These samples contained greater abundances of Fe-rich brucite and iowaite, which have been inferred to record hydrothermal alteration temperatures of <200°C (Kahl et al., 2015), perhaps as low as 50°C (Heling and Schwarz, 1992). As theoretical isotope fractionation calculations predict (Schauble, 2007), these data suggest that lower alteration temperatures produce lighter Tl isotope compositions. However, given that Tl isotopes in the Si-poor samples are similar to both clastic sediments and altered oceanic crust subducted beneath the Mariana arc, we cannot unambiguously use Tl isotopes to further constrain the origin of lighter ε^{205}Tl in some of the investigated samples.

The heavy ε^{205}Tl value of a rodingite from Conical seamount is consistent with rodingitization via sediment-derived serpentinization fluids, which highlights that mass transfer between sediments, mafic- and ultramafic lithologies takes place at shallow levels within the forearc mantle. As such, metasomatic mass transfer at temperatures up to 300 °C must be taken into account when assessing the elemental budgets of subduction zones. In particular, fluid mobile elements like B, Pb, Tl, Cs and others could potentially be stripped from specific lithologies in the subducting plate to a degree that significantly affects the elemental and isotopic mass balance of the total slab. Ultimately these processes could affect not just chemical and isotopic signatures translated into arc lavas, but also the magnitude of mass transfer of these elements into the mantle.

The results presented here are suggestive of systematic Tl isotope changes in response to chemical and physical changes in the hydrothemal alteration environment of the Mariana forearc. However, given the relatively small dataset presented, we caution that further work is needed before the processes controlling the relationships between Tl isotopes, LOI and silica content can be accurately determined.

7. Acknowledgements

We thank three anonymous reviewers and editor Mike Bickle for insightful comments and suggestions that helped improve this manuscript. We gratefully acknowledge the WSU GeoAnalytical Lab for their excellent help with the XRF analysis. This study used samples recovered during the Ocean Drilling Program. This study was funded by NSF grants EAR-1119373 and -1427310 to SGN, NSF grant OCE-1059534 to FK and a grant from the WHOI Deep Ocean Exploration Institute to FK and SGN.

8. References

Alt, J.C., Shanks, W.C., 2006. Stable isotope compositions of serpentinite seamounts in the Mariana forearc: Serpentinization processes, fluid sources and sulfur metasomatism. Earth Planet. Sci. Lett. 242, 272-285.

Bach, W., Jöns, N., Klein, F., 2013. Metasomatism Within the Ocean Crust, in: Harlov, D.E., Austrheim, H. (Eds.), Metasomatism and the Chemical Transformation of Rock. Springer, pp. 253-288.

Bach, W., Klein, F., 2009. The petrology of seafloor rodingites: Insights from geochemical reaction path modeling. Lithos 112, 103-117.

Barnes, J.D., Sharp, Z.D., Fischer, T.P., 2008. Chlorine isotope variations across the Izu-Bonin-Mariana arc. Geology 36, 883-886.

Beard, J.S., Frost, B.R., Fryer, P., McCaig, A., Searle, R., Ildefonse, B., Zinin, P., Sharma, S.K., 2009. Onset and Progression of Serpentinization and Magnetite Formation in Olivine-rich Troctolite from IODP Hole U1309D. J. Petrol. 50, 387-403.

Byrne, R.H., 2002. Inorganic speciation of dissolved elements in seawater: the influence of pH on concentration ratios. Geochemical Transactions 3, 11-16.

Coggon, R.M., Rehkämper, M., Atteck, C., Teagle, D.A.H., Alt, J.C., Cooper, M.J., 2014. Mineralogical and Microbial Controls on Thallium Uptake During Hydrothermal Alteration of the Upper Ocean Crust. Geochim. Cosmochim. Acta. 144, 25-42.

Coleman, R.G., 1963. Serpentinites, rodingites, and tectonic inclusions in alpine-type mountain chains. Geological Society of America Special Paper 73.

Coleman, R.G., 1977. Ophiolites: Ancient oceanic lithosphere? Springer, New York.

Evans, B.W., 2004. The serpentine multisystem revisited: chrysotile is metastable. International Geology Review 46, 479-506.

Flegal, A.R., Patterson, C.C., 1985. Thallium concentrations in seawater. Mar. Chem. 15, 327-331.

Frost, B.R., Beard, J.S., 2007. On silica activity and serpentinization. J. Petrol. 48, 1351-1368.

Frost, B.R., Beard, J.S., McCaig, A., Condliffe, E., 2008. The formation of micro-rodingites from IODP Hole U1309D: Key to understanding the process of serpentinization. J. Petrol. 49, 1529-1588.

Frost, R.L., Erickson, K.L., 2004. Thermal decomposition of natural iowaite. Journal of Thermal Analysis and Calorimetry 78, 367-373.

Fryer, P., 2012. Serpentinite mud volcanism: observations, processes, and implications. Annual Review of Marine Science 4, 345-373.

Fryer, P., Ambos, E.L., Hussong, D.M., 1985. Origin and emplacement of Mariana Forearc seamounts. Geology 13, 774-777.

Fryer, P., Gharib, J., Ross, K., Savov, I.P., Mottl, M.J., 2006. Variability in serpentinite mudflow mechanisms and sources: ODP drilling results on Mariana forearc seamounts. Geochem. Geophys. Geosyst. 7, Q08014.

Fryer, P., Saboda, K.L., Johnson, L.E., Mackay, M.E., Moore, G.F., Stoffers, P., 1990. Conical Seamount: SeaMARC II, Alvin Submersible, and Seismic-Reflection Studies. Proceedings ODP, Initial Reports 12, 69-80.

Fryer, P., Wheat, C.G., Mottl, M.J., 1999. Mariana blueschist mud volcanism: Implications for conditions within the subduction zone. . Geology 27, 103-106.

Hein, J.R., Koschinsky, A., Bau, M., Manheim, F.T., Kang, J.-K., Roberts, L., 2000. Cobalt-rich ferromanganese crusts in the Pacific, in: Cronan, D.S. (Ed.), Handbook of Marine Mineral Deposits. CRC Press, Boca Raton, pp. 239-280.

Heinrichs, H., Schulz-Dobrick, B., Wedepohl, K.H., 1980. Terrestrial Geochemistry of Cd, Bi, Tl, Pb, Zn and Rb. Geochim. Cosmochim. Acta. 44, 1519-1533.

Heling, D., Schwarz, A., 1992. Iowaite in serpentinite muds at sites 778, 779, 780 and 784: a possible cause for the low chlorinity of pore waters. Proc. ODP Sci. Results 125, 313-323.

Hulme, S.M., Wheat, C.G., Fryer, P., Mottl, M.J., 2010. Pore water chemistry of the Mariana serpentinite mud volcanoes: A window to the seismogenic zone. . Geochem. Geophys. Geosyst. 11, 29.

Hyndman, R.D., Peacock, S.M., 2003. Serpentinization of the forearc mantle. . Earth Planet. Sci. Lett. 212, 417-432.

Johnson, D.M., Hooper, P.R., Conrey, R.M., 1997. XRF Analysis of Rocks and Minerals for Major and Trace Elements on a Single Low Dilution Li-tetraborate Fused Bead. Advances in X-ray Analysis 41, 843-867.

Johnson, L.E., 1992. Mafic clasts in serpentine seamounts: Petrology and geochemistry of a diverse crustal suite from the outer Mariana forearc. Proc. ODP Sci. Results 125, 401-413.

Johnson, L.E., Fryer, P., 1990. The first evidence for MORB-like lavas from the outer Mariana forearc: geochemistry, petrography and tectonic implications. Earth Planet. Sci. Lett. 100, 304-316.

Kahl, W.-A., Jöns, N., Bach, W., Klein, F., Alt, J.C., 2015. Ultramafic clasts from the South Chamorro serpentine mud volcano reveal a polyphase serpentinization history of the Mariana forearc mantle. Lithos 227, 1-20.

Klein, F., Bach, W., Humphris, S.E., Kahl, W.-A., Jöns, N., Moskowitz, B., Berquó, T., 2014. Magnetite in seafloor serpentinite - Some like it hot. Geology 42, 135-138.

Klein, F., Bach, W., Jöns, N., McCollom, T.M., Moskowitz, B., Berquó, T., 2009. Iron partitioning and hydrogen generation during serpentinization of abyssal peridotites from 15°N on the Mid-Atlantic Ridge. Geochim. Cosmochim. Acta. 73, 6868-6893.

Klein, F., Bach, W., McCollom, T.M., 2013. Compositional Controls on Hydrogen Generation During Serpentinization of Ultramafic Rocks. . Lithos 178, 55-69.

Klein, F., Grozeva, N.G., Seewald, J.S., McCollom, T.M., Humphris, S.E., Moskowitz, B., Berquo, T.S., Kahl, W.A., 2015. Experimental constraints on fluid-rock reactions during incipient serpentinization of harzburgite. American Mineralogist 100, 991-1002.

Kodolanyi, J., Pettke, T., Spandler, C., Kamber, B.S., Gmeling, K., 2012. Geochemistry of Ocean Floor and Fore-arc Serpentinites: Constraints on the Ultramafic Input to Subduction Zones. J. Petrol. 53, 235-270.

Maekawa, H., Shozul, M., Ishii, T., Fryer, P., Pearce, J.A., 1993. Blueschist Metamorphism in an Active Subduction Zone. Nature 364, 520-523.

Makishima, A., Nakamura, E., 2006. Determination of major, minor and trace elements in silicate samples by ICP-QMS and ICP-SFMS applying isotope dilution-internal standardisation (ID-IS) and multi-stage internal standardisation. Geostand. Geoanal. Res. 30, 245-271.

Metz, S., Trefry, J.H., 2000. Chemical and mineralogical influences on concentrations of trace metals in hydrothermal fluids. Geochim. Cosmochim. Acta. 64, 2267-2279.

Mével, C., Stadoumi, C., 1996. Hydrothermal alteration of the upper mantle section at Hess Deep. Proc. ODP Sci. Results 147, 293-309.

Mottl, M.J., Wheat, C.G., Fryer, P., Gharib, J., Martin, J.B., 2004. Chemistry of springs across the Mariana forearc shows progressive devolatilization of the subducting plate. Geochim. Cosmochim. Acta. 68, 4915-4933.

Murata, K., Maekawa, H., Yokose, H., Yamamoto, K., Fujioka, K., Ishii, T., Chiba, H., Wada, Y., 2009. Significance of serpentinization of wedge mantle peridotites beneath Mariana forearc. Geosphere 5, 90-104.

Nielsen, S.G., Mar-Gerrison, S., Gannoun, A., LaRowe, D., Klemm, V., Halliday, A.N., Burton, K.W., Hein, J.R., 2009a. Thallium isotope evidence for a permanent increase in marine organic carbon export in the early Eocene. Earth Planet. Sci. Lett. 278, 297-307.

Nielsen, S.G., Rehkämper, M., 2011. Thallium isotopes and their application to problems in earth and environmental science, in: Baskaran, M. (Ed.), Handbook of Environmental Isotope Geochemistry. Springer, pp. 247-270.

Nielsen, S.G., Rehkämper, M., Baker, J., Halliday, A.N., 2004. The precise and accurate determination of thallium isotope compositions and concentrations for water samples by MC-ICPMS. Chem. Geol. 204, 109-124.

Nielsen, S.G., Rehkämper, M., Brandon, A.D., Norman, M.D., Turner, S., O'Reilly, S.Y., 2007. Thallium isotopes in Iceland and Azores lavas - Implications for the role of altered crust and mantle geochemistry. Earth Planet. Sci. Lett. 264, 332-345.

Nielsen, S.G., Rehkämper, M., Halliday, A.N., 2006a. Large thallium isotopic variations in iron meteorites and evidence for lead-205 in the early solar system. Geochim. Cosmochim. Acta. 70, 2643-2657.

Nielsen, S.G., Rehkämper, M., Norman, M.D., Halliday, A.N., Harrison, D., 2006b. Thallium isotopic evidence for ferromanganese sediments in the mantle source of Hawaiian basalts. Nature 439, 314-317.

Nielsen, S.G., Rehkämper, M., Porcelli, D., Andersson, P., Halliday, A.N., Swarzenski, P.W., Latkoczy, C., Gunther, D., 2005. Thallium isotope composition of the upper continental crust and rivers - An investigation of the continental sources of dissolved marine thallium. Geochim. Cosmochim. Acta. 69, 2007-2019.

Nielsen, S.G., Rehkämper, M., Teagle, D.A.H., Alt, J.C., Butterfield, D., Halliday, A.N., 2006c. Hydrothermal fluid fluxes calculated from the isotopic mass balance of thallium in the ocean crust. Earth Planet. Sci. Lett. 251, 120-133.

Nielsen, S.G., Shimizu, N., Lee, C.T.A., Behn, M., 2014. Chalcophile behavior of thallium during MORB melting and implications for the sulfur content of the mantle. Geochem. Geophys. Geosyst. 15, 4905-4919.

Nielsen, S.G., Wasylenki, L.E., Rehkämper, M., Peacock, C.L., Xue, Z., Moon, E.M., 2013. Towards an understanding of thallium isotope fractionation during adsorption to manganese oxides. Geochim. Cosmochim. Acta. 117, 252-265.

Nielsen, S.G., Williams, H.M., Griffin, W.L., O'Reilly, S.Y., Pearson, N., Viljoen, F., 2009b. Thallium isotopes as a potential tracer for the origin of cratonic eclogites. Geochim. Cosmochim. Acta. 73, 7387-7398.

Pabst, S., Zack, T., Savov, I.P., Ludwig, T., Rost, D., Tonarini, S., Vicenzi, E.P., 2012. The fate of subducted oceanic slabs in the shallow mantle: Insights from boron isotopes and light element composition of metasomatized blueschists from the Mariana forearc. Lithos 132, 162-179.

Prytulak, J., Nielsen, S.G., Plank, T., Barker, M., Elliott, T., 2013. Assessing the utility of thallium and thallium isotopes for tracing subduction zone inputs to the Mariana arc. Chem. Geol. 345, 139-149.

Rehkämper, M., Frank, M., Hein, J.R., Halliday, A., 2004. Cenozoic marine geochemistry of thallium deduced from isotopic studies of ferromanganese crusts and pelagic sediments. Earth Planet. Sci. Lett. 219, 77-91.

Rehkämper, M., Frank, M., Hein, J.R., Porcelli, D., Halliday, A., Ingri, J., Liebetrau, V., 2002. Thallium isotope variations in seawater and hydrogenetic, diagenetic, and hydrothermal ferromanganese deposits. Earth Planet. Sci. Lett. 197, 65-81.

Rehkämper, M., Halliday, A.N., 1999. The precise measurement of Tl isotopic compositions by MC-ICPMS: Application to the analysis of geological materials and meteorites. Geochim. Cosmochim. Acta. 63, 935-944.

Sakai, R., Kusakabe, M., Noto, M., Ishii, T., 1990. Origin of waters responsible for serpentinization of the Izu-Ogasawara-Mariana forearc seamounts in view of hydrogen and oxygen isotope ratios. Earth Planet. Sci. Lett. 100, 291-303.

Salisbury, M.H., Shinohara, M., Richter, C., Araki, E., Barr, S.R., D'Antonio, M., Dean, S.M., Diekmann, B., Edwards, K.M., Fryer, P.B., Gaillot, P.J., Hammon III, W.S., Hart, D., Januszczak, N., Komor, S.C., Kristensen, M.B., Lockwood, J.P., Mottl, M.J., Moyer, C.L., Nakahigashi, K., Savov, I.P., Su, X., Wei, K.-Y., Yamada, T., 2002. Volume 195 initial reports. Proceedings ODP, Initial Reports 195.

Savov, I.P., Ryan, J.G., D'Antonio, M., Fryer, P., 2007. Shallow slab fluid release across and along the Mariana arc-basin system: Insights from geochemistry of serpentinized peridotites from the Mariana fore arc. J. Geophys. Res.-Solid Earth 112.

Schauble, E.A., 2007. Role of nuclear volume in driving equilibrium stable isotope fractionation of mercury, thallium, and other very heavy elements. Geochim. Cosmochim. Acta. 71, 2170-2189.

Shannon, R.D., 1976. Revised effective ionic radii and systematic studies of interatomic distances in halides and chalcogenides. Acta Crystallographica A32, 751-767.

Shaw, D.M., 1952. The geochemistry of thallium. Geochim. Cosmochim. Acta. 2, 118-154.

Teagle, D.A.H., Alt, J.C., Bach, W., Halliday, A.N., Erzinger, J., 1996. Alteration of upper ocean crust in a ridge-flank hydrothermal upflow zone: Mineral, chemical, and isotopic constraints from hole 896A. Proc. ODP Sci. Results 148, 119-150.

Wedepohl, K.H., 1995. The composition of the continental crust. Geochim. Cosmochim. Acta. 59, 1217-1232.

Figure captions:

Figure 1: *Simplified schematic illustration of thallium isotope compositions encountered in a forearc tectonic setting compared with those measured for Mariana forearc serpentinites and rodingite. Note that this illustration is not to scale. Moreover, because the extent and nature of the forearc crust is not well constrained, it is omitted here for the sake of simplicity. Deep faults may or may not connect directly with the décollement. Rodingite formation, which is favored during serpentinization at temperatures lower than ca. 300°C (Bach et al., 2013; Bach and Klein, 2009), probably takes place away from the décollement in Si-depleted environments. At the décollement where the expelled fluid is in equilibrium with Si-rich slab components, such as sediments or oceanic crust, rodingitization seems unlikely. Instead blackwall alteration of mafic lithologies and steatitization of peridotite seems more likely (Bach et al., 2013). Thallium isotope data from (Coggon et al., 2014; Nielsen et al., 2006b; Nielsen et al., 2006c; Nielsen et al., 2013; Rehkämper et al., 2004; Rehkämper et al., 2002) and this study. Diagram is modified from Fryer et al. (2006).*

Figure 2: *Thin section photomicrograph mosaics (a, b, e, f), confocal Raman maps (c, d) and back scatter electron image (g) of strongly serpentinized peridotite. a) Peridotite (Sample 1200A 3R-1W, 3-7 cm) is altered to lizardite (Lz) and minor magnetite (Mag), whereas brucite (Brc) is present only in trace amounts. Spinel (Spl) is virtually unaltered. Late chrysotile veins cut across earlier veins and mesh texture (cf. Kahl et al., in revision). b) Sample 1200A 13R-1W, 121-124 cm. Olivine (Ol) is altered to lizardite, brucite and iowaite (Iow), whereas magnetite did not form. c) Confocal Raman map showing Fe-bearing brucite (blue), iowaite (red) and lizardite (green) in mesh texture. Note that iowaite partly replaces brucite. Raman bands at* $444cm^{-1}$, $527cm^{-1}$ *and* $690cm^{-1}$ *were chosen to represent brucite, iowaite, and lizardite, respectively. The latter was confirmed using O-H stretching band at* $3708cm^{-1}$. *d) Confocal Raman map (colors same as in c) showing a late vein of Fe-rich brucite, which is partly replaced by iowaite. e) Rodingitized diabase (Sample 779A 31R-2W, 85-87cm) is composed of secondary diopside (Di), hydrogarnet (Grt), and minor chlorite, in addition to a number of trace phases. f) Strongly serpentinized, brucite-poor harzburgite (sample 779A 10R-2W, 51-53cm). g) Partly serpentinized olivine in brucite-free mesh texture, consisting of lizardite and Ni-Fe rich opaque phases.*

Figure 3: *Thallium isotope compositions of serpentinites and rodingite from the Mariana forearc plotted against a) loss on ignition (LOI), b)* SiO_2 *and c) Tl concentrations. Fields for the composition of the harzburgite protolith before hydrothermal alteration are also shown in b) and c). The Tl concentration of harzburgite is estimated based on our measurement of one harzburgite from Eifel, Germany, combined with the most recent estimate of the average Tl content of the upper mantle of 0.5 ng/g (Nielsen et al., 2014). We also took into account that Tl is an incompatible trace element and therefore harzburgites from the normal depleted mantle are likely to exhibit Tl concentrations significantly lower than the average upper mantle. It is evident that lower LOI and Tl concentrations and higher* SiO_2 *concentrations characterize the isotopically heavier samples. These relationships imply that different alteration conditions produced serpentinites with different Tl isotope compositions (see text for details).*

Table 1: Thallium isotope and concentration data for BHVO-1

Split number	ε^{205}Tl	[Tl] (ng/g)
1	-3.45	39.5
2	-3.52	39.2
3	-3.23	35.6
4	-3.42	34.3
5	-3.51	36.8
6	-3.29	33.1
7	-3.85	38.2
8	-3.45	35.6
9	-4.10	39.2
10	-3.35	37.3
Average	*-3.5*	*36.9*
2sd	0.5	4.4

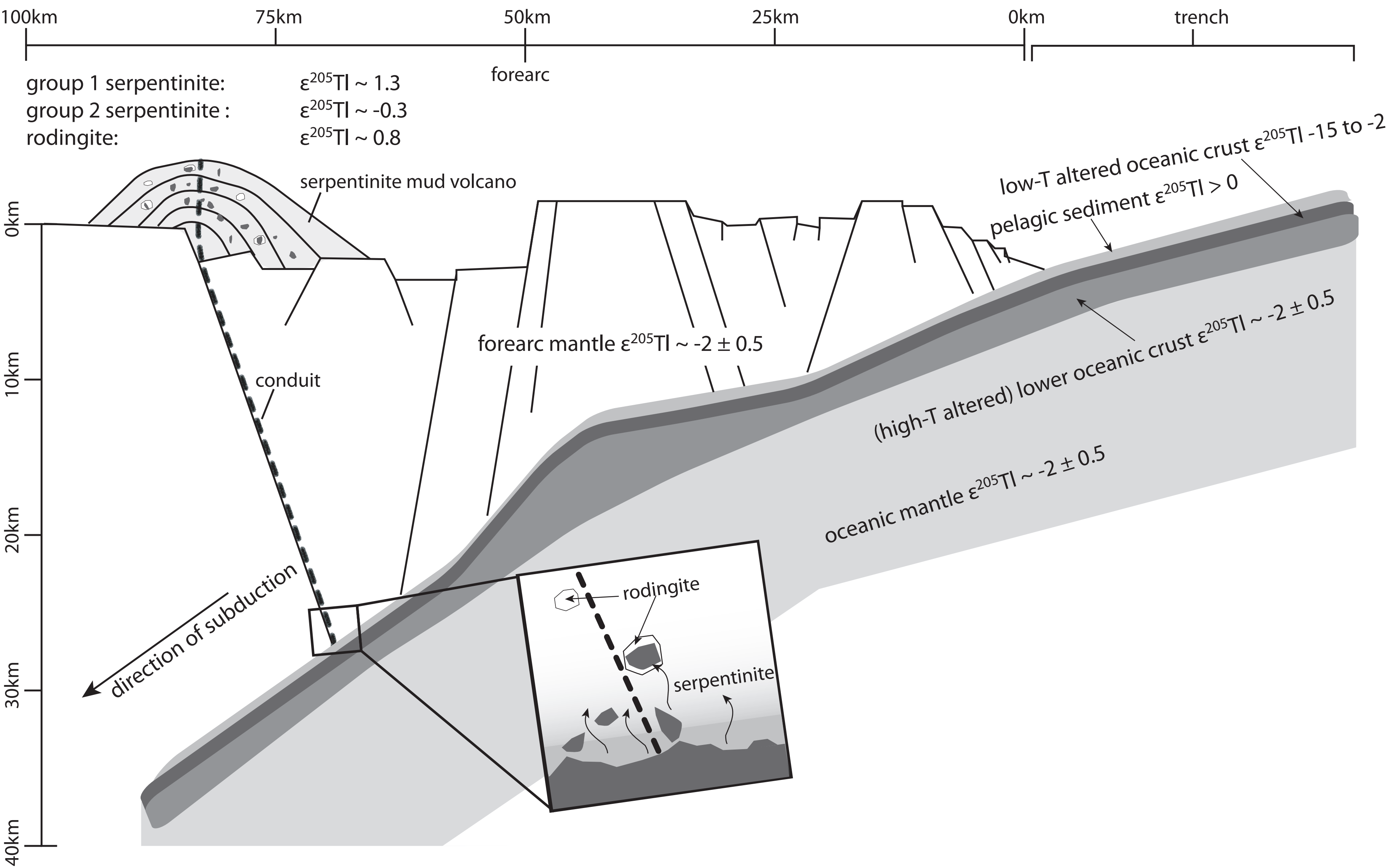
100km
75km
50km
25km
0km
trench
forearc
group 1 serpentinite: ε205Tl ~ 1.3
group 2 serpentinite : ε205Tl ~ -0.3
rodingite: ε205Tl ~ 0.8
serpentinite mud volcano
low-T altered oceanic crust ε205Tl -15 to -2
pelagic sediment ε205Tl > 0
forearc mantle ε205Tl ~ -2 ± 0.5
(high-T altered) lower oceanic crust ε205Tl ~ -2 ± 0.5
oceanic mantle ε205Tl ~ -2 ± 0.5
conduit
0km
10km
20km
30km
40km
direction of subduction
rodingite
serpentinite

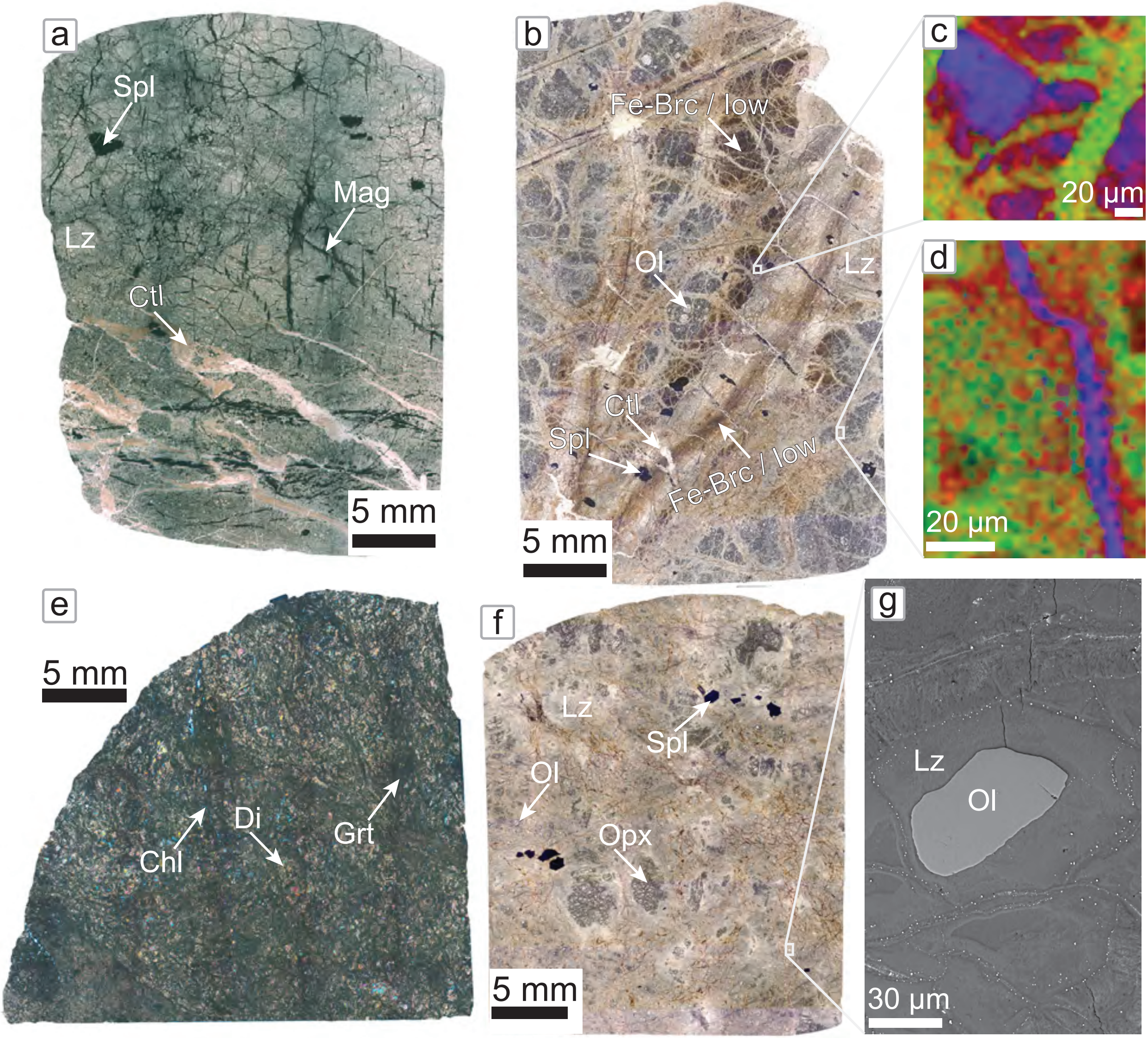
a
Spl
Mag
Lz
Ctl
5 mm
b
Fe-Brc / low
Ol
Lz
Ctl
Spl
Fe-Brc / low
5 mm
c
20 μm
d
20 μm
e
5 mm
Chl
Di
Grt
f
Lz
Spl
Ol
Opx
5 mm
g
Lz
Ol
30 μm

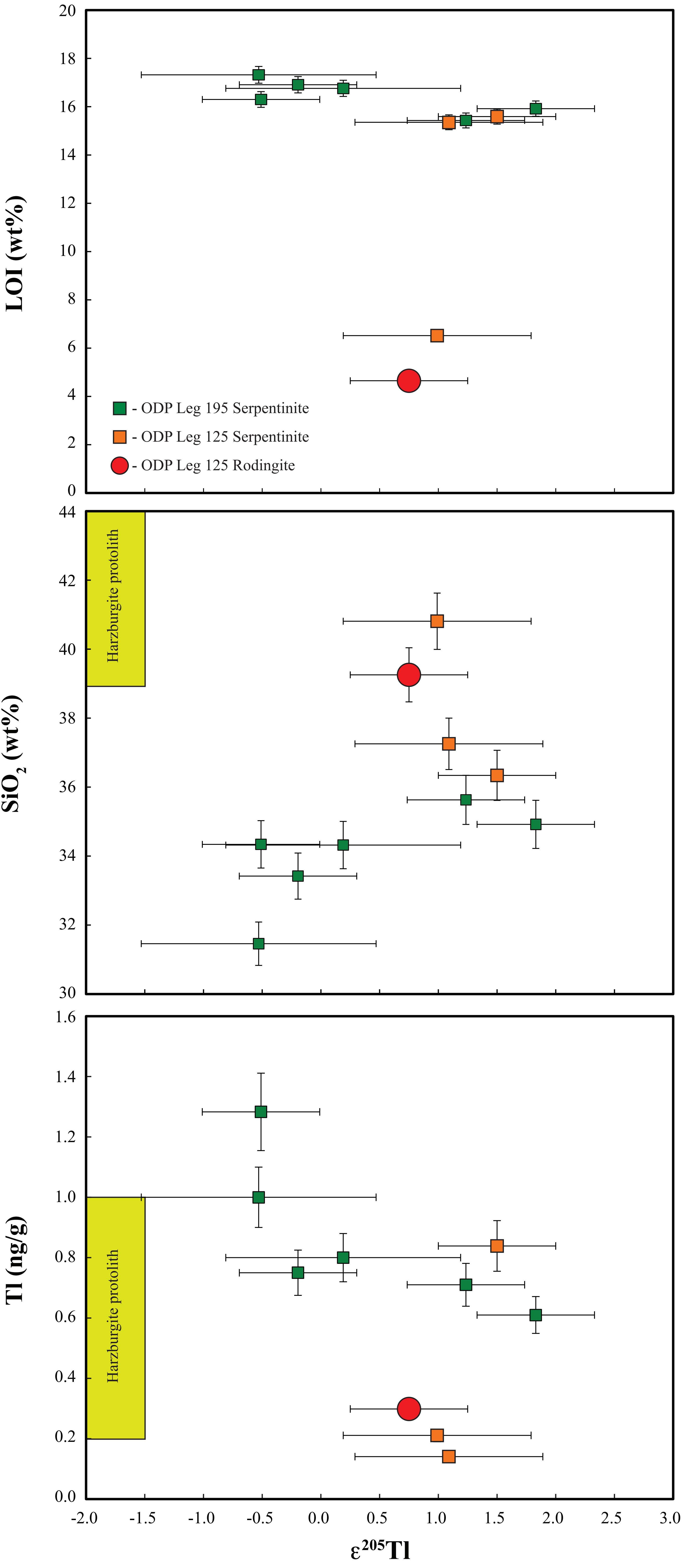
LOI (wt%)
20
18
16
14
12
10
8
6
4
2
0
🟩 - ODP Leg 195 Serpentinite
🟧 - ODP Leg 125 Serpentinite
● - ODP Leg 125 Rodingite
SiO2 (wt%)
44
42
40
38
36
34
32
30
Harzburgite protolith
Tl (ng/g)
1.6
1.4
1.2
1.0
0.8
0.6
0.4
0.2
0.0
Harzburgite protolith
-2.0
-1.5
-1.0
-0.5
0.0
0.5
1.0
1.5
2.0
2.5
3.0
ε205Tl